ISSN: 0067-2904

Effect of the slip conditions with rotation, wall properties and heat transfer on peristaltic transport MHD

Hatem Nahi[1*], Mustafa Hatem[2]

[1] *Department of Mathematics, minister's office, Ministry of High Education and Scientific Research, Baghdad, Iraq.*

[2] *Department of Mathematics, Privet al Esraa University, Baghdad, Iraq.*

Received: 27/1/2024 Accepted: 8/4/2024 Published: 30/3/2025

Abstract

In this study, we look into how the peristaltic flow MHD is affected by rotation, heat transfer, elasticity wall characteristics, and slip conditions. For simplification, the governing equations, infinite wavelength and small Reynolds numbers have been used to study the Newtonian fluid in a porous canal. Heat transport, elasticity, rotation, and slip conditions are taken into account. The Brinkman number, Hartman number, and other parameters are evaluated to observe their effects on the stream function, temperature, velocity, and coefficient of heat transfer. The results indicate that when these parameters are varied, more trapped boluses develop. Figures and graphs discuss and illustrate the impact of various values on these factors. The MATHEMATICA software has been used to compute numerical results.

Keywords: Elasticity wall, Peristaltic Transport, Slip condition, coefficient of heat transfer, Brinkman number, Rotation.

تأثير شروط الانزلاق مع الدوران وكذلك خصائص الجدار مع انتقال الحرارة على النقل التمعجيMHD

حاتم ناهي[*1] ، مصطفى حاتم[2]

[1] قسم الرياضيات, مكتب الوزير, وزارة التعليم بالعالي والبحث العلمي, بغداد, العراق

[2] قسم الرياضيات, جامعة الاسراء الاهلية, بغداد, العراق

الخلاصة

في هذه الدراسة، سننظر في كيفية تأثر التدفق التمعجي MHD بالدوران، وانتقال الحرارة، وخصائص جدار المرونة، وظروف الانزلاق. لتبسيط المعادلات الحاكمة، تم دراسة السائل النيوتوني في قناة مسامية تحت شروط الطول الموجي الطويل وعدد رينولدز الصغير. يتم أخذ ظروف النقل الحراري والمرونة والدوران والانزلاق في الاعتبار. يتم تقييم رقم برينكمان ورقم هارتمان والمعلمات الأخرى لمعرفة مدى تأثيرها على درجة الحرارة والسرعة ومعامل نقل الحرارة ودالة التدفق. وتشير النتائج إلى أنه عندما تتغيير هذه المعلمات، تتطور المزيد من الجرعات المحاصرة. تناقش سلسلة الأشكال وتوضح بيانياً تأثير القيم المختلفة لهذه العوامل. تم استخدام برنامج MATHEMATICA لحساب النتائج العددية.

*Email: ha19652010@yahoo.com

1. Introduction

The process of fluid transformation that is known as peristaltic transport is brought about by a sinusoidal wave propagating through the canal walls. The peristaltic phenomenon is widely observed in a variety of industrial, engineering, and biological contexts. Among these are the flow of urine from the kidney to the bladder, food swallowing through the esophagus, blood circulation in the tiny blood arteries, ovum migration in the fallopian tubes, and other processes. The concept of peristaltic pumping has been used in the construction of several contemporary mechanical systems to move fluids without the need for internal moving parts that is similar to the heart-lung machine blood push. Numerous works are performed in this filed, we will mention some of them below. In [1], the authors analytically and numerically investigated and focuses on how the magnetic field and wall slip circumstances affect the peristaltic transport of the Newtonian fluid in an asymmetric canal. The effects of the heat transfer and wall slip conditions on MHD peristaltic flow with infinite wavelength and small Reynolds number have been used to investigate the Newtonian fluid in a porous canal that has properties of an elastic parapet [2]. Under assumption that the infinite wavelength and small Reynolds number, the authors [3] examined and investigated the effects of heat transfer, elasticity parapet characteristics, and parapet slip conditions on the peristaltic transport of conduction Bingham fluid in asymmetric canal. This study presents an analytical analysis of the movement of the Williamson fluid with heat transfer via a tube with slip at borders and complaisant parapet properties. A theoretical model that is roughly developed is made of flexible, complaisant, spring backed tubing with parapets that is chosen to motion in a sinusoidal wave pattern [4]. In [5], the authors analytically provided a study of the mathematical model that describes the slip peristaltic low of a nanofluid and they also analytically examined in this study. For the temperature distribution and nanoparticle concentration, precise expressions were inferred. The study in [6] examines how magnetohydrodynamics (MHD) affects Ree-Eyring fluid's peristaltic transport in a rotating frame. The findings deal with applying each of the Ree-Eyring fluid's governing equations methodically (analytically), furthermore with the axial and secondary velocities, auxiliary stream flow rate, and bolus. The authors [7] served applications as inspiration for their study which models the peristaltic flow of a Ree–Eyring liquid via a homogeneous complaisant canal while taking into account the effects of changing thermal conductivity and viscosity. In [8], the main goal of the research project is to investigate blood circulation in the small vessels by accounting for wall properties such as thickness, slip, and varying thermal conductivity. Under the presumptions of long wavelength and low Reynolds number, authors in [9] have been studied how the elasticity of the flexible parapets affects the MHD peristaltic flow of the Newtonian fluid in a two-dimensional porous canal with heat transfer. The peristaltic flow of nanofluid in a conduit with compliant walls is also examined in this paper. The Brownian motion and thermophoresis effects are discussed in [10]. The analytical study of peristaltic flow and heat transmission in a 2-dimensional plane tube with complaisant parapet properties and slip at the borders is also investigated in this work. A roughly constructed theoretical model is made of flexible, compliant walled pipe with a spring backing, selected to move in a sinusoidal wave pattern [11]. The article discusses the impact of mass and heat transfer on the (MHD) peristaltic flow in a planar canal with complaisant parapets. Maxwell's incompressible fluid is contained in a porous medium [12]. The work provides a thorough analysis of the novel concept of porous medium in conjunction with an altered version of Darcy's law. Ree-Eyring fluid models have been used as the foundation for research on nanofluid flow. The flow crosses the recurved canal is produced by the peristaltic waves generated by the contraction and relaxation of smooth muscle. Additionally, fluctuating viscosity and magnetohydrodynamics are involved in the flow kinetics [13]. The authors examined how heat and mass transfer affects the Casson fluid's hydro-magnetic

peristaltic flow through an asymmetric channel in a rotating inclined system [14]. The study in [15] examines the effects of rotation, magnetic field, and several variables, including flow rate, density, viscosity, Grashof, Bingham, and Brinkman numbers regarding the peristaltic transport of viscoplastic fluid through the porous material using mixed convection heat transfer analysis. The study in [16] examines the effects of rotational variation and other variables on the peristaltic flow of mixed convection in an incompressible viscoplastic fluid. In asymmetrical two-dimensional canal, the authors also examined some variables including density, viscosity, flow velocity, tapering, Grashof number, Bingham number, and Brinkman number regarding the examination of mixed convection heat transfer for peristaltic viscoplastic fluid transport taking into account the following assumptions the long wavelengths, small Reynolds numbers, peristaltic transport in asymmetric border walls, tapering horizontal canals, and asymmetric canals to have varying wave and phase amplitudes. In [17], the study describes how Bingham's fluid behaves peristaltically in an asymmetric channel made of porous material. It is anticipated that the fluid will be sensitive to a strong, inclined magnetic field and flow through a porous media. The work in [18] examines the rotation and heat transfer during the peristaltic flow of a micropolar fluid in a vertical symmetric channel. The infinite wavelength approximation and small Reynolds number flow analysis have been also developed. The Bingham plastic fluid's peristaltic flow is examined for relation to heat transfer, rotation, and an induced magnetic field in two dimensions. The relationship between rotating momentum, energy, and the induced magnetic field equations [19]. The peristaltic flow of the Powell-Eyring fluid through a porous media with heat transfer in an inclined asymmetric channel with an inclining magnetic field is studied for relation to the influence of the rotation variable and other variables [20]. The impact of nonlinear thermal radiation and magnetic force on the peristaltic transport of a hybrid bio-nanofluid in a symmetric canal with a porous medium is discussed [21]. One of the most important characteristics of fluid flow in various mechanical scenarios is the ability to display slip at the solid barrier. Consequently, the purpose of the article in [22] is to clarify the slip effect that results from unrestricted convection and rotational viscous fluid flow across an elongated plate with mass and heat transfer when a continuous magnetic field passes through a porous media. The authors [23] use an incompressible non-Newtonian fluid to investigate the effects of the rotation of an inclined magnetic felid and an inclined symmetric channel with slip condition on peristaltic transport. Consideration is also given to the slip conditions for concentration and heat transfer. In [24], a fluid-porous composite system with rigid-rigid boundaries that are protected from temperature and concentration is the subject of the study on triple diffusive magneto convection. In a two-layers system, the impact of a heat source and temperature gradient on the Brinkman-Bènard Triple-Diffusive magneto-Marangoni (BBTDMM) convection is examined [25].

In this paper, we will display how influence the slip, rotation and effect of heat transfer on peristaltic transport magnetohydrodynamics with elastic wall, some properties are also studied in this research.

2. Mathematical equations

We examine the Newtonian viscous fluid's flow via a uniformly thick and two-dimensional conduit. It is assumed that the channel's walls are elastic and act as if they are an extending membrane that is being subjected to moving, reasonably amplitude sinusoidal waves. The mathematical form of the canal wall is given as follows:

$$y = \eta(\bar{X}, \bar{t}) = d + \bar{m}\bar{X} + a\, sin\,(\frac{2\pi}{\lambda})(\bar{X} - c\bar{t});\ Where, \bar{m} \ll 1. \quad (1)$$

The following are the predominant equations of motion for the present problem:
The continuity equation is:

$$\frac{\partial \bar{U}}{\partial \bar{X}} + \frac{\partial \bar{V}}{\partial \bar{Y}} = 0. \quad (2)$$

The momentum equation on the X-axis is given by

$$\rho\left(\frac{\partial \bar{U}}{\partial \bar{t}} + \bar{U}\frac{\partial \bar{U}}{\partial \bar{X}} + \bar{V}\frac{\partial \bar{U}}{\partial \bar{Y}}\right) - \rho\Omega\left(\Omega\bar{U} + 2\frac{\partial \bar{V}}{\partial \bar{t}}\right) = -\frac{\partial \bar{P}}{\partial \bar{X}} + \mu[\frac{\partial^2 \bar{U}}{\partial \bar{X}^2} + \frac{\partial^2 \bar{U}}{\partial \bar{Y}^2}] - \sigma {B_0}^2 \bar{U} - \frac{\mu}{k}\bar{U}. \quad (3)$$

The momentum equation on the Y-axis is as follows:

$$\rho\left(\frac{\partial \bar{V}}{\partial \bar{t}} + \bar{U}\frac{\partial \bar{V}}{\partial \bar{X}} + \bar{V}\frac{\partial \bar{V}}{\partial \bar{Y}}\right) - \rho\Omega\left(\Omega\bar{U} - 2\frac{\partial \bar{V}}{\partial \bar{t}}\right) = -\frac{\partial \bar{P}}{\partial \bar{Y}} + \mu[\frac{\partial^2 \bar{V}}{\partial \bar{X}^2} + \frac{\partial^2 \bar{V}}{\partial \bar{Y}^2}] - \frac{\mu}{k}\bar{V}. \quad (4)$$

The energy equation is given by

$$\rho C_\rho\left(\frac{\partial \bar{T}}{\partial \bar{t}} + \bar{U}\frac{\partial \bar{T}}{\partial \bar{X}} + \bar{V}\frac{\partial \bar{T}}{\partial \bar{Y}}\right) = \gamma\left(\frac{\partial^2 \bar{T}}{\partial \bar{X}^2} + \frac{\partial^2 \bar{T}}{\partial \bar{Y}^2}\right) + \upsilon[2\left[\left(\frac{\partial \bar{U}}{\partial \bar{X}}\right)^2 + \left(\frac{\partial \bar{V}}{\partial \bar{Y}}\right)^2\right] + \left(\frac{\partial \bar{U}}{\partial \bar{Y}} + \frac{\partial \bar{V}}{\partial \bar{X}}\right)^2]. \quad (5)$$

Where $\bar{U}$ and $\bar{V}$ denote the velocity components along the $\bar{X}$ and $\bar{Y}$ directions, respectively, the density is represented by ρ, the fluid's coefficient of viscosity is represented by μ, $\bar{P}$ is the pressure, d is the canal's mean half-width, the amplitude is represented by a, λ is the wavelength, c is the wave's phase speed, the canal's dimensional asymmetric is denoted by $\bar{m}$, σ represents the fluid's electrical conductivity, B_0 is used for the magnetic field, C_ρ is the particular heat at a fixed volume, υ is the fluid's kinematic viscosity, γ represents the fluid's thermal conductivity, T is the fluid's temperature, the parameter for permeability is k, and **Ω** is the rotation parameter.

The dominant equation of motion for the plastic parapet is as follows:

$$L^*(\eta) = P - P_0. \quad (6)$$

Where L^* is an operator, it is used to depict how a stretched membrane moves when viscous damping forces are applied, it is given by:

$$L^* = -\tau\frac{\partial^2}{\partial \bar{X}^2} + m_1\frac{\partial^2}{\partial \bar{t}^2} + C\frac{\partial}{\partial \bar{t}} \quad (7)$$

Continuity of the stress at $y = \pm\eta$ and using x-momentum equation, this yields the following:

$$\frac{\partial}{\partial \bar{X}}L^*(\eta) = \frac{\partial \bar{P}}{\partial \bar{X}} = \rho\Omega\left(\Omega\bar{U} + 2\frac{\partial \bar{V}}{\partial \bar{t}}\right) + \mu(\frac{\partial^2 \bar{U}}{\partial \bar{X}^2} + \frac{\partial^2 \bar{U}}{\partial \bar{Y}^2}) - \rho\left(\frac{\partial \bar{U}}{\partial \bar{t}} + \bar{U}\frac{\partial \bar{U}}{\partial \bar{X}} + \bar{V}\frac{\partial \bar{U}}{\partial \bar{Y}}\right) - \sigma {B_0}^2\bar{U} - \frac{\mu}{k}\bar{U}, \quad (8)$$

$$u = \mp h\frac{\partial \bar{U}}{\partial \bar{Y}} \; at \; y = \pm\eta = \pm[d + \bar{m}\bar{X} + asin\left(\frac{2\pi}{\lambda}\right)(\bar{X} - ct)], \quad (9)$$

$$\bar{T} = T_0 \; on \; y = -\eta, \; \bar{T} = T_1 \; on \; y = \eta. \quad (10)$$

In this case, τ represents the membrane's elastic tension, mass per unit area is denoted by m, C is the viscosity dampen might coefficient, P_0 is the pressure that the muscles are applying to the wall's exterior, and the parameter for dimensional slip is h. We assume $y = 0$.

The stream function ψ in a way that $\boldsymbol{u} = \frac{\partial \psi}{\partial y}, \boldsymbol{v} = -\frac{\partial \psi}{\partial x}$, and non-dimensional quantities:

$$\bar{X}=\frac{x}{\lambda},\bar{Y}=\frac{y}{d},\bar{\psi}=\frac{\psi}{\lambda},\theta=\frac{T-T_0}{T_1-T_0},\bar{\eta}=\frac{\eta}{d},\bar{p}=\frac{d^2}{c\lambda\mu}p,K=\frac{k}{d^2},\bar{U}=\frac{u}{c},\bar{V}=\frac{v}{\delta c},\delta=\frac{d}{\lambda},R_e=\frac{\rho cd}{\mu},\gamma=\frac{k}{d^2},\ M=\sqrt{\frac{\sigma}{\mu}d\ B_0},P_r=\frac{\rho\upsilon C_p}{k},E_c=\frac{c^2}{C_p(T_1-T_0)},\varepsilon=\frac{a}{d},m=\frac{\lambda\bar{m}}{d},\beta=\frac{h}{d},\bar{t}=\frac{ct}{\lambda},E_1=\frac{-\tau d^3}{\mu c\lambda^3},E_2=\frac{cm_1d^3}{\mu\lambda^3},E_3=\frac{cd^3}{\mu\lambda^2},A=\frac{\rho d^2\Omega^2}{\mu}. \quad (11)$$

Where δ and ε are the dimensionless geometric parameters R_e, P_r, E_c are the Reynolds number, Prandtl number, Eckert number, respectively. E_1, E_2, E_3 *and* M are the dimensionless elasticity parameters and Hartman number, m and β are the asymmetric parameter and slip parameter or Knudsen number, respectively.
Using equations (1-10) with help equation (11), we get

$$R_e\delta\left[\frac{\partial^2\psi}{\partial t\partial y}+\frac{\partial\psi}{\partial y}\frac{\partial^2\psi}{\partial x\partial y}-\frac{\partial\psi}{\partial x}\frac{\partial^2\psi}{\partial y^2}\right]=-\frac{\partial p}{\partial x}+\delta^2\frac{\partial^3\psi}{\partial x^2\partial y}+\frac{\partial^3\psi}{\partial y^3}+\left(A-M^2-\frac{1}{K}\right)\frac{\partial\psi}{\partial y}, \quad (12)$$

$$R_e\delta^3\left[\frac{\partial^2\psi}{\partial t\partial x}+\frac{\partial\psi}{\partial y}\frac{\partial^2\psi}{\partial x^2}-\frac{\partial\psi}{\partial x}\frac{\partial^2\psi}{\partial x\partial y}\right]=-\frac{\partial p}{\partial y}+\delta^2\left[\delta^2\frac{\partial^3\psi}{\partial x^3}+\frac{\partial^3\psi}{\partial x\partial y^2}\right]+\delta^2[A-\frac{1}{K}]\frac{\partial\psi}{\partial y}, \quad (13)$$

$$R_e\delta\left[\frac{\partial\theta}{\partial t}+\frac{\partial\psi}{\partial y}\frac{\partial\theta}{\partial x}-\frac{\partial\psi}{\partial x}\frac{\partial\theta}{\partial y}\right]=\frac{1}{P_r}\left(\delta^2\frac{\partial^2}{\partial x^2}+\frac{\partial^2}{\partial y^2}\right)\theta+$$
$$E_c\left[4\delta^2\left(\frac{\partial^2\psi}{\partial x\partial y}\right)^2+\left(\frac{\partial^2\psi}{\partial y^2}-\delta^2\frac{\partial^2\psi}{\partial x^2}\right)^2\right], \quad (14)$$

$$\frac{\partial\psi}{\partial y}=\mp\beta\frac{\partial^2\psi}{\partial y^2}\quad at\ y=\ \pm\eta=\pm[1+mx+\varepsilon\sin 2\pi\ (x-t)], \quad (15)$$

$$\delta^2\frac{\partial^3\psi}{\partial x^2\partial y}+\frac{\partial^3\psi}{\partial y^3}-R_e\delta[\left[\frac{\partial^2\psi}{\partial t\partial y}+\frac{\partial\psi}{\partial y}\frac{\partial^2\psi}{\partial x\partial y}-\frac{\partial\psi}{\partial x}\frac{\partial^2\psi}{\partial y^2}\right]+\left(A-M^2-\frac{1}{K}\right)\frac{\partial\psi}{\partial y}$$
$$=[E_1\frac{\partial^3}{\partial x^3}+E_2\frac{\partial^3}{\partial x\partial t^2}+E_3\frac{\partial^2}{\partial x\partial t}]\eta \quad (16)$$

Additionally, it is presumable that the streamline's zero magnitude at the line y=0, i.e.
$$\psi(0)=0, \quad (17)$$
$$\theta=0\ on\ y=\ -\eta;\ \ \theta=1\ \ on\ y=\eta$$

The solution to the problem

The following equations can be used to determine the solution by applying the infinite wavelength approximation, ignoring the wave number, and using the small Reynolds number (12-16) that

$$\frac{\partial p}{\partial x}=\ \frac{\partial^3\psi}{\partial y^3}+(A-M^2-\frac{1}{K})\frac{\partial\psi}{\partial y}, \quad (19)$$

$$-\frac{\partial p}{\partial x}=0 \quad (20)$$

As shown by equation (20), p is not a function of y.

$$\frac{1}{P_e}\frac{\partial^2\theta}{\partial y^2}+E_c(\frac{\partial^2\psi}{\partial y^2})^2=0. \quad (21)$$

The compatibility equation on differentiation equation (19) with regard to y is as follows:

$$\frac{\partial^4\psi}{\partial y^4}+(A-N)\frac{\partial^2\psi}{\partial y^2}=0 \quad (22)$$

Where $N=\sqrt{M^2+\frac{1}{K}}$.

Equation (16) gives:

$$\frac{\partial^3\psi}{\partial y^3}+(A-N)\frac{\partial\psi}{\partial y}=E_1\frac{\partial^3\eta}{\partial x^3}+E_2\frac{\partial^3\eta}{\partial x\partial t^2}+E_3\frac{\partial^2\eta}{\partial x\partial t}. \quad (23)$$

with boundary conditions (15, 17) and (23) in closed form gives the following:

$$\psi = -\frac{4\pi^2(1-e^{\sqrt{A-k}y}-e^{\sqrt{A-k}(\eta1+\eta2)}+e^{\sqrt{A-k}(-y+\eta1+\eta2)}+e^{\sqrt{A-k}\eta2}y(\sqrt{A-k}+A\beta-k\beta)+e^{\sqrt{A-k}\eta1}y(\sqrt{A-k}-A\beta+k\beta))\epsilon(2(\mathrm{E1+E2})\pi\mathrm{Cos}[2\pi(t-x)]+\mathrm{E3Sin}[2\pi(t-x)])}{(A-k)^{3/2}(e^{\sqrt{A-k}\eta1}(-1+\sqrt{A-k}\beta)-e^{\sqrt{A-k}\eta2}(1+\sqrt{A-k}\beta))}$$

Substituting the value of ψ into equation (21) and the temperature and subject to condition (18), we get:

$$\theta = -\frac{1}{4(A-k)}\mathrm{BR}\left(\frac{16e^{-2\sqrt{A-k}y+2\sqrt{A-k}(\eta1+\eta2)}\pi^4\epsilon^2(2(\mathrm{E1+E2})\pi\mathrm{Cos}[2\pi(t-x)]+\mathrm{E3Sin}[2\pi(t-x)])^2}{(A-k)(e^{\sqrt{A-k}\eta1}(1-\sqrt{A-k}\beta)+e^{\sqrt{A-k}\eta2}(1+\sqrt{A-k}\beta))^2}+\right.$$
$$\frac{64e^{\sqrt{A-k}(\eta1+\eta2)}\pi^4y^2\epsilon^2(2(\mathrm{E1+E2})\pi\mathrm{Cos}[2\pi(t-x)]+\mathrm{E3Sin}[2\pi(t-x)])(2(\mathrm{E1+E2})\pi\mathrm{Cos}[2\pi(-t+x)]+\mathrm{E3Sin}[2\pi(t-x)])}{(e^{\sqrt{A-k}\eta1}(-1+\sqrt{A-k}\beta)-e^{\sqrt{A-k}\eta2}(1+\sqrt{A-k}\beta))(e^{\sqrt{A-k}\eta1}(1-\sqrt{A-k}\beta)+e^{\sqrt{A-k}\eta2}(1+\sqrt{A-k}\beta))}+$$
$$\left.\frac{16e^{2\sqrt{A-k}y}\pi^4\epsilon^2(2(\mathrm{E1+E2})\pi\mathrm{Cos}[2\pi(-t+x)]+\mathrm{E3Sin}[2\pi(t-x)])^2}{(A-k)(e^{\sqrt{A-k}\eta1}(-1+\sqrt{A-k}\beta)-e^{\sqrt{A-k}\eta2}(1+\sqrt{A-k}\beta))^2}\right)-\frac{1}{4(\eta1-\eta2)(A-k)}y(4A-4k+$$
$$\frac{16\mathrm{BR}e^{2\sqrt{A-k}(\eta1+\eta2)}(-e^{-2\eta1\sqrt{A-k}}+e^{-2\eta2\sqrt{A-k}})\pi^4\epsilon^2(2(\mathrm{E1+E2})\pi\mathrm{Cos}[2\pi(t-x)]+\mathrm{E3Sin}[2\pi(t-x)])^2}{(A-k)(e^{\sqrt{A-k}\eta1}(1-\sqrt{A-k}\beta)+e^{\sqrt{A-k}\eta2}(1+\sqrt{A-k}\beta))^2}-$$
$$\frac{64\mathrm{BR}e^{\sqrt{A-k}(\eta1+\eta2)}(\eta1-\eta2)(\eta1+\eta2)\pi^4\epsilon^2(2(\mathrm{E1+E2})\pi\mathrm{Cos}[2\pi(t-x)]+\mathrm{E3Sin}[2\pi(t-x)])(2(\mathrm{E1+E2})\pi\mathrm{Cos}[2\pi(-t+x)]+\mathrm{E3Sin}[2\pi(t-x)])}{(e^{\sqrt{A-k}\eta1}(-1+\sqrt{A-k}\beta)-e^{\sqrt{A-k}\eta2}(1+\sqrt{A-k}\beta))(e^{\sqrt{A-k}\eta1}(1-\sqrt{A-k}\beta)+e^{\sqrt{A-k}\eta2}(1+\sqrt{A-k}\beta))}-$$
$$\left.\frac{16\mathrm{BR}(e^{2\eta1\sqrt{A-k}}-e^{2\eta2\sqrt{A-k}})\pi^4\epsilon^2(2(\mathrm{E1+E2})\pi\mathrm{Cos}[2\pi(-t+x)]+\mathrm{E3Sin}[2\pi(t-x)])^2}{(A-k)(e^{\sqrt{A-k}\eta1}(-1+\sqrt{A-k}\beta)-e^{\sqrt{A-k}\eta2}(1+\sqrt{A-k}\beta))^2}\right)-$$
$$\frac{1}{4(\eta1-\eta2)(A-k)}\left(\mathrm{BR}\eta2\left(\frac{16e^{-2\eta1\sqrt{A-k}+2\sqrt{A-k}(\eta1+\eta2)}\pi^4\epsilon^2(2(\mathrm{E1+E2})\pi\mathrm{Cos}[2\pi(t-x)]+\mathrm{E3Sin}[2\pi(t-x)])^2}{(A-k)(e^{\sqrt{A-k}\eta1}(1-\sqrt{A-k}\beta)+e^{\sqrt{A-k}\eta2}(1+\sqrt{A-k}\beta))^2}+\right.\right.$$
$$\frac{64e^{\sqrt{A-k}(\eta1+\eta2)}\eta1^2\pi^4\epsilon^2(2(\mathrm{E1+E2})\pi\mathrm{Cos}[2\pi(t-x)]+\mathrm{E3Sin}[2\pi(t-x)])(2(\mathrm{E1+E2})\pi\mathrm{Cos}[2\pi(-t+x)]+\mathrm{E3Sin}[2\pi(t-x)])}{(e^{\sqrt{A-k}\eta1}(-1+\sqrt{A-k}\beta)-e^{\sqrt{A-k}\eta2}(1+\sqrt{A-k}\beta))(e^{\sqrt{A-k}\eta1}(1-\sqrt{A-k}\beta)+e^{\sqrt{A-k}\eta2}(1+\sqrt{A-k}\beta))}+$$
$$\left.\left.\frac{16e^{2\eta1\sqrt{A-k}}\pi^4\epsilon^2(2(\mathrm{E1+E2})\pi\mathrm{Cos}[2\pi(-t+x)]+\mathrm{E3Sin}[2\pi(t-x)])^2}{(A-k)(e^{\sqrt{A-k}\eta1}(-1+\sqrt{A-k}\beta)-e^{\sqrt{A-k}\eta2}(1+\sqrt{A-k}\beta))^2}\right)+\right.$$
$$\eta1\left(-\frac{16\mathrm{BR}e^{-2\eta2\sqrt{A-k}+2\sqrt{A-k}(\eta1+\eta2)}\pi^4\epsilon^2(2(\mathrm{E1+E2})\pi\mathrm{Cos}[2\pi(t-x)]+\mathrm{E3Sin}[2\pi(t-x)])^2}{(A-k)(e^{\sqrt{A-k}\eta1}(1-\sqrt{A-k}\beta)+e^{\sqrt{A-k}\eta2}(1+\sqrt{A-k}\beta))^2}-\right.$$
$$\frac{16\mathrm{BR}e^{2\eta2\sqrt{A-k}}\pi^4\epsilon^2(2(\mathrm{E1+E2})\pi\mathrm{Cos}[2\pi(-t+x)]+\mathrm{E3Sin}[2\pi(t-x)])^2}{(A-k)(e^{\sqrt{A-k}\eta1}(-1+\sqrt{A-k}\beta)-e^{\sqrt{A-k}\eta2}(1+\sqrt{A-k}\beta))^2}-4(A-k)(1+$$
$$\left.\left.\frac{16\mathrm{BR}e^{\sqrt{A-k}(\eta1+\eta2)}\eta2^2\pi^4\epsilon^2(2(\mathrm{E1+E2})\pi\mathrm{Cos}[2\pi(t-x)]+\mathrm{E3Sin}[2\pi(t-x)])(2(\mathrm{E1+E2})\pi\mathrm{Cos}[2\pi(-t+x)]+\mathrm{E3Sin}[2\pi(t-x)])}{(A-k)(e^{\sqrt{A-k}\eta1}(-1+\sqrt{A-k}\beta)-e^{\sqrt{A-k}\eta2}(1+\sqrt{A-k}\beta))(e^{\sqrt{A-k}\eta1}(1-\sqrt{A-k}\beta)+e^{\sqrt{A-k}\eta2}(1+\sqrt{A-k}\beta))}\right)\right)$$

Where $Br = E_c\, P_r$ is the Brinkman number.

The following formula provides the wall's coefficient of the heat transfer [2]:

$$Z = \eta_x\, \theta_y\,. \qquad (24)$$

4. Discussion of the results

The coefficient of the heat transmission, temperature, velocity, and stream function distributions of these variables wit respect to β, m, K, M, and Ω are discussed in this section.

4.1 Velocity profile

We examine the velocity distribution in relation to several variables. The velocity profile is clearly seen in Figure 1 from A to E. It was observed that the rising values of β, and M indicate a decrease in the velocity, however, the rising values of (m, K, Ω) indicate an increase in the velocity.

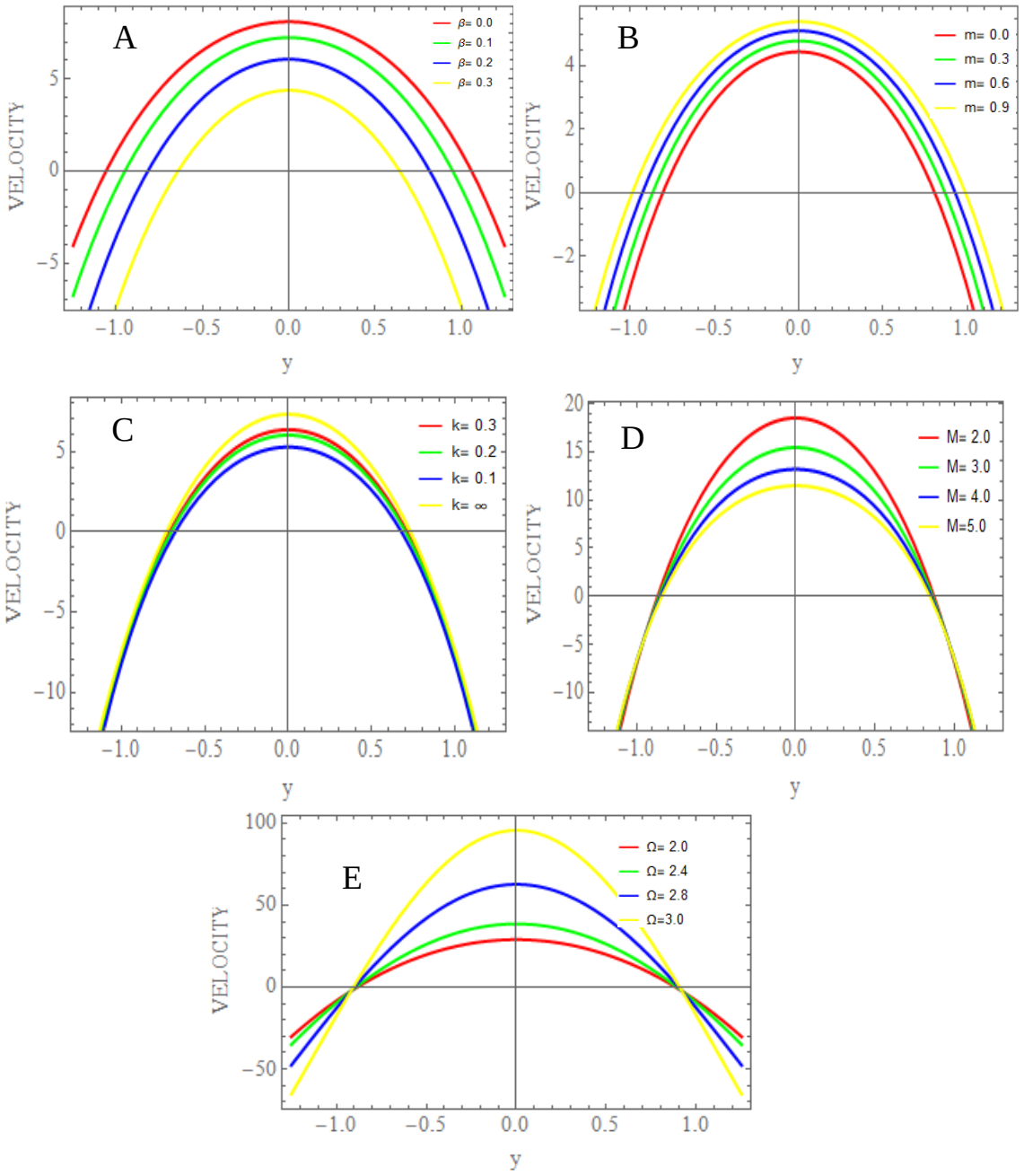

Figure1: Velocity distributions (x=0.2, t= 0.1). **(A)** E1=0.1, E2=0.5, E3=0.5,$\varepsilon = 0.1, \Omega = 0.2$, m=0.0, M=2.0,$\mu = 2.0, \rho = 0.9, K = 2.0$). **(B)** E1=0.8, E2=0.5, E3=0.4, $\varepsilon = 0.1, \Omega = 0.2, \beta$=0.2, M=3.0, $\mu = 2.0, \rho = 0.9, K = 2.0$). **(C)** E1=0.5, E2=0.5, E3=0.1, $\varepsilon = 0.2, \Omega = 0.2, \beta$=0.3, M=2.0, $\mu = 2.0, \rho = 0.9, m = 0.1$). **(D)** E1=0.2, E2=0.7, E3=0.15, $\varepsilon = 0.15, \Omega = 0.2, \beta$=0.2, K=2.0, $\mu = 2.0, \rho = 0.9, m = 0.1$). **(E)** E1=0.2, E2=0.7, E3=0.1, $\varepsilon = 0.15, \beta$=0.2, M=2.0, $\mu = 2.0, \rho = 0.9, m = 0.1, K = 2.0$).

4.2 The temperature profile

This section discusses the behaviour of temperature when varying the values of the variable parameters. The behaviour of the temperature variable is shown in Figure 2. This is evident from Figure 2 (A-F). As the values of (β, m, k, **Ω**, BR) increase, the temperature rises. It falls when the Hartman number (M) increases.

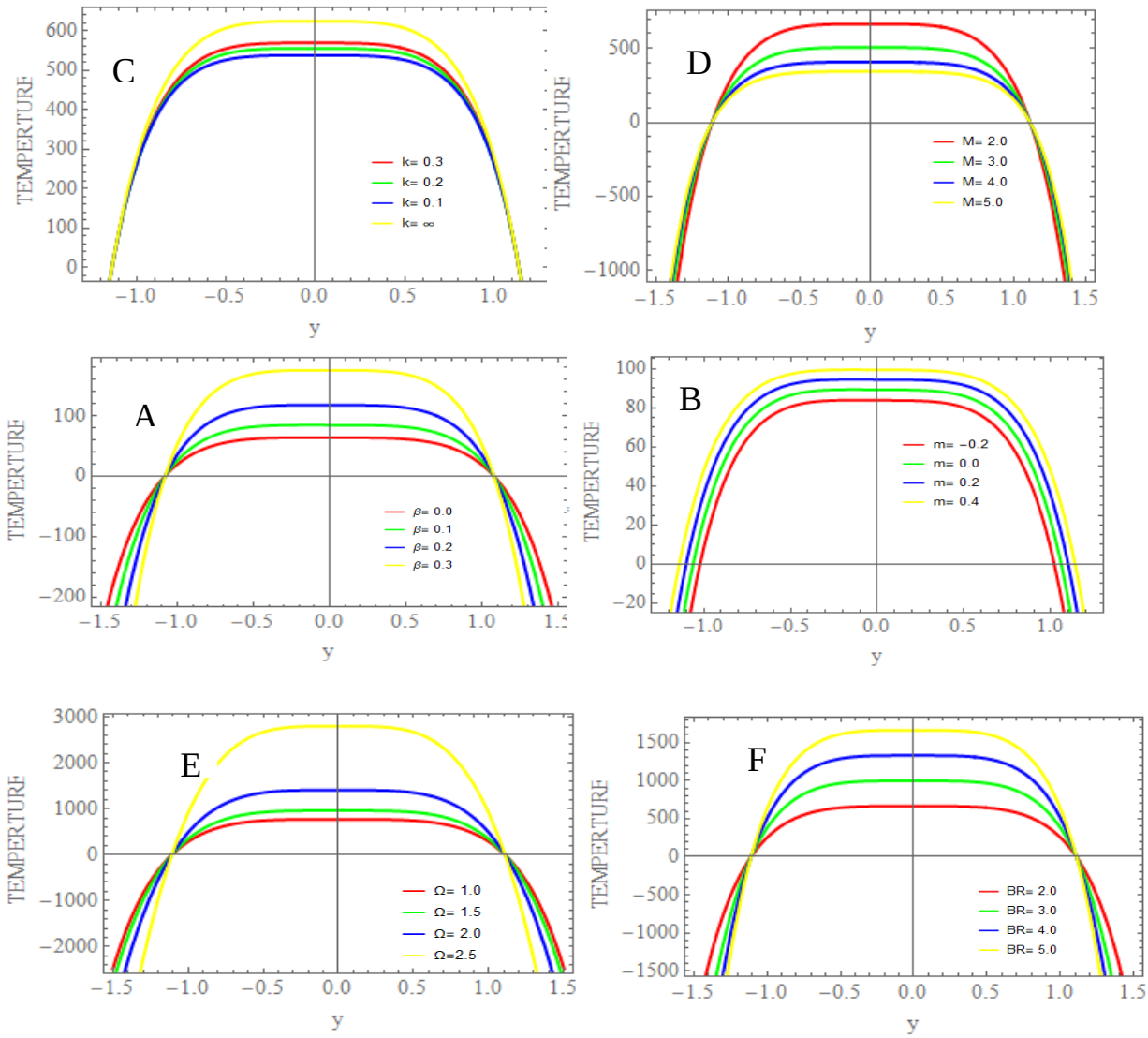

Figure. 2 Temperature distributions (x=0.2, t= 0.1**). (A)** E1=0.5, E2=0.5, E3=0.5,$\varepsilon = 0.1, \Omega = 0.2$, m=0.1, BR=3.0, M=2.0,$\mu = 2.0, \rho = 0.9, K = 2.0$). **(B)** E1=0.8, E2=0.5, E3=0.4, $\varepsilon = 0.1, \Omega = 0.2, \beta$=0.2, BR=4.0, M=3.0, $\mu = 2.0, \rho = 0.9, K = 2.0$). **(C)** E1=0.5, E2=0.5, E3=0.1, $\varepsilon = 0.2, \Omega = 0.2, \beta$=0.3, M=2.0, $\mu = 2.0, \rho = 0.9, m = 0.1$). **(D)** E1=0.2, E2=0.7, E3=0.1BR=5.0,, $\varepsilon = 0.15, \Omega = 0.2, \beta$=0.2, K=2.0, $\mu = 2.0, \rho = 0.9, m = 0.1$). **(E)** E1=0.2, E2=0.7, E3=0.1, $\varepsilon = 0.15, \beta$=0.2, M=2.0, $\mu = 2.0, \rho = 0.9, BR = 2.0, m = 0.1, K = 2.0$). **(F)** E1=0.2, E2=0.7, E3=0.1, $\varepsilon = 0.15, \beta$=0.2, M=2.0, $\mu = 2.0, \rho = 0.9, m = 0.1, K = 2.0, \Omega = 0.2$).

4.3 The coefficient of the heat transfer

The fluctuation in the heat transmission coefficient (Z) for different values of the relevant parameters is analysed and showed in Figure 3. It is noted that the heat transfer coefficient exhibits oscillating behaviour as a result of peristalsis. Presented in Figs.3 from (A–F) for illustration. We have seen that an increase in the values of (β, K, **Ω**, BR) indicates a rise in the coefficient of heat transfer; on the other hand, an increase in the value of (M) implies the opposite.

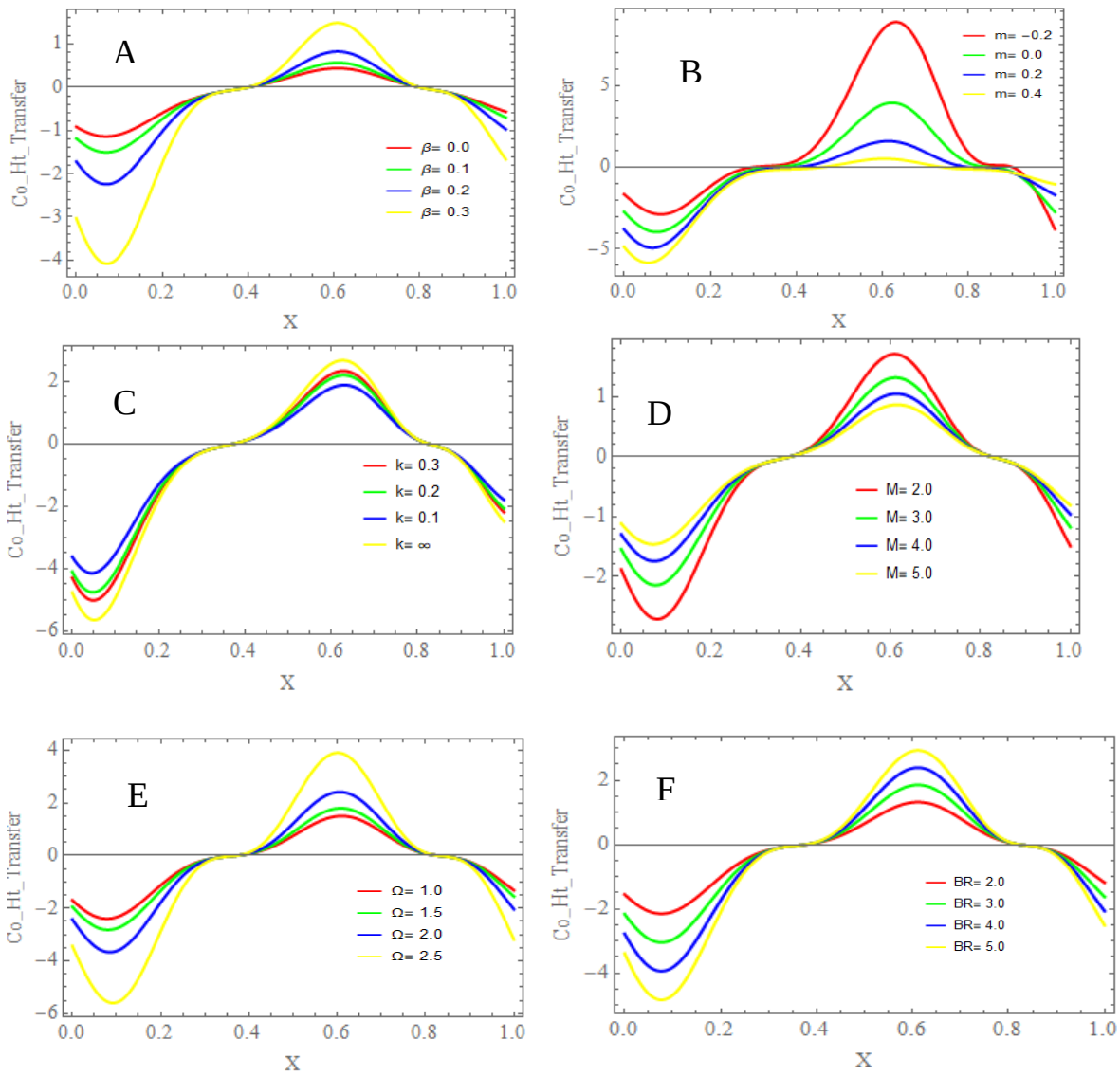

Figure. 3 Coefficient of Heat Transfer (y=0.4, t= 0.1). **(A)** E1=0.4, E2=0.1, E3=0.1,$\varepsilon = 0.1, \Omega = 0.2$, m=0.2, BR=3.0, M=3.0,$\mu = 2.0, \rho = 0.9, K = 2.0$). **(B)** E1=1.2, E2=0.5, E3=0.1, $\varepsilon = 0.1, \Omega = 0.2, \beta$=0.1, BR=2.0, M=5.0, $\mu = 2.0, \rho = 0.9, K = 2.0$). **(C)** E1=0.3, E2=0.1, E3=0.1, $\varepsilon = 0.2, \Omega = 0.2, \beta$=0.1, BR=3.0, M=4.0, $\mu = 2.0, \rho = 0.9, m = 0.2$). **(D)** E1=0.5, E2=0.1, E3=0.1,BR=2.0, $\varepsilon = 0.1, \Omega = 0.2, \beta$=0.2, K=0.5, $\mu = 2.0, \rho = 0.9, m = 0.1$). **(E)** E1=0.5, E2=0.1, E3=0.1, $\varepsilon = 0.1, \beta$=0.2, M=3.0, $\mu = 2.0, \rho = 0.9, BR = 2.0, m = 0.1, K = 0.5$). **(F)** E1=0.5, E2=0.1, E3=0.1, $\varepsilon = 0.1, \beta$=0.2, M=3.0, $\mu = 2.0, \rho = 0.9, m = 0.1, K = 0.5, \Omega = 0.2$).

4.4 The stream function

Trapping is an intriguing peristaltic transport event. In this part, we examine the effects of various parameters on the fluid's steam function. Figures (4-8) clearly show how the slip parameter and rotation affect fluid entrapment. With an increase in the slip parameter, we find that streamlines shut loops producing a cellular flow motif in the canal and increase trapped bolus, Additionally, we observe that when the slip parameter is increased, the number of bolus is decreased (see Figure 4 from (a) to (d)). The quantity and size of the trapped bolus that is apparent in Figure 5 (a-d) rise as the value of m increases. Furthermore, one can see that in Figure 6(a-b), the size of the trapped bolus grows with increasing k and more trapped bolus occurs with increasing k. Figure 7(a-d) illustrates how M affects trapping and shows

how the number of boluses increases as the M parameter value increases. Additionally, when the rotation value increases, some boluses are implied, and the bolus at the left of the channel expands (see Figure 8(a-d). Additionally, it starts when M rises in value.

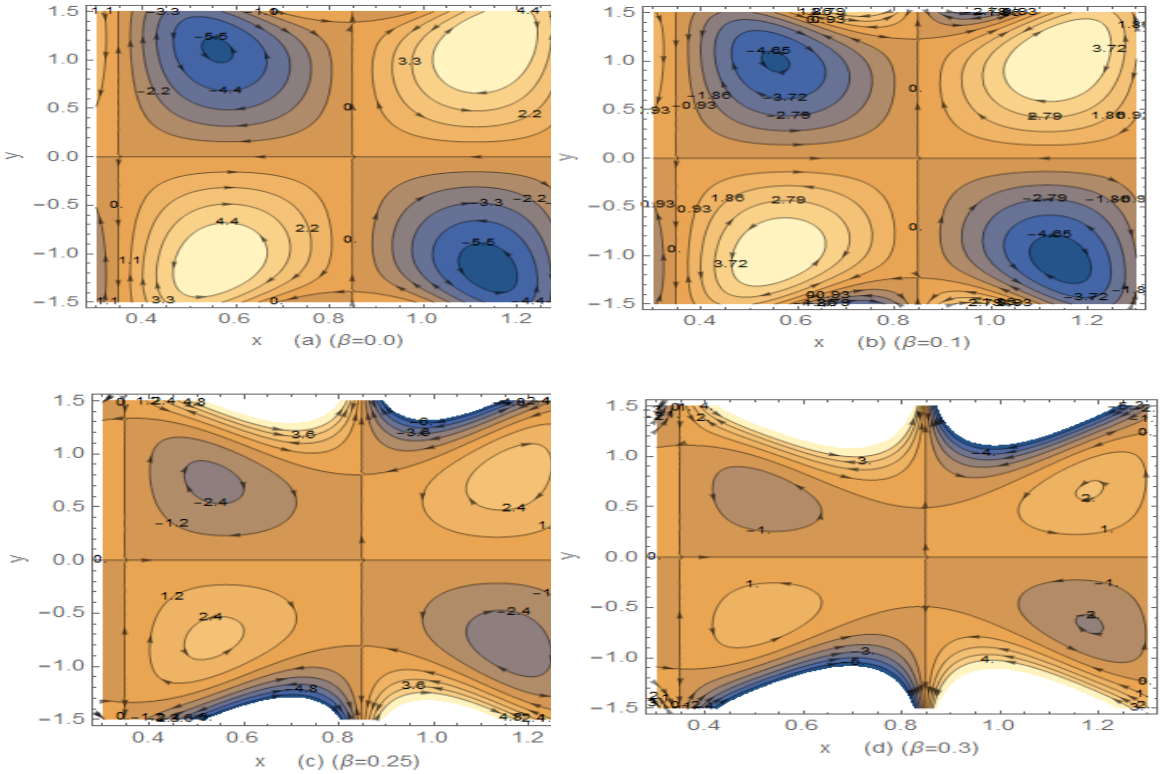

Figure. 4: Stream Function (t=0.1, E1=0.6, E2=0.4, E3=0.1, ϵ=0.2, M=4, k=0.05, m=0.1, Ω=0.2, μ=2.0, ρ=0.9).

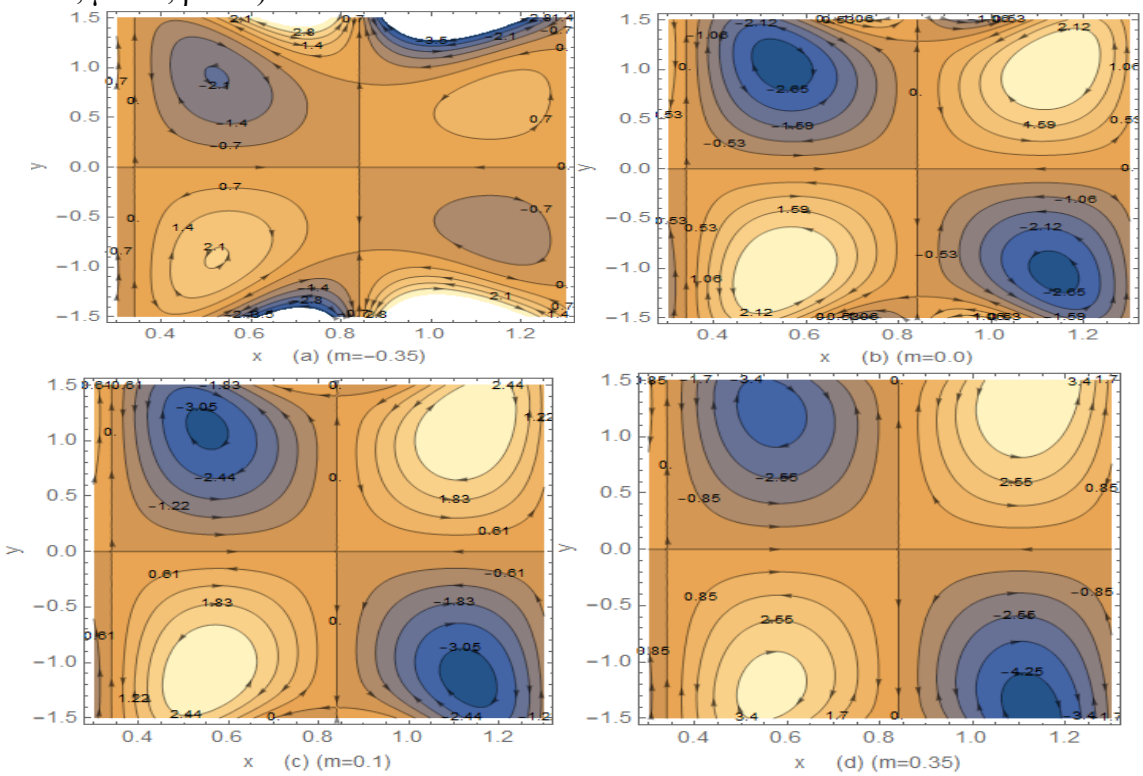

Figure 5: Stream Function $(t = 0.1, \mathrm{E1} = 0.4, \mathrm{E2} = 0.1, \mathrm{E3} = 0.2,\ \epsilon = 0.2,\ M = 4,\ \mathrm{k} = 0.1,\ \mu = 2.0,\ \rho = 0.9,\ \beta = 0.0, \Omega = 0.2.$

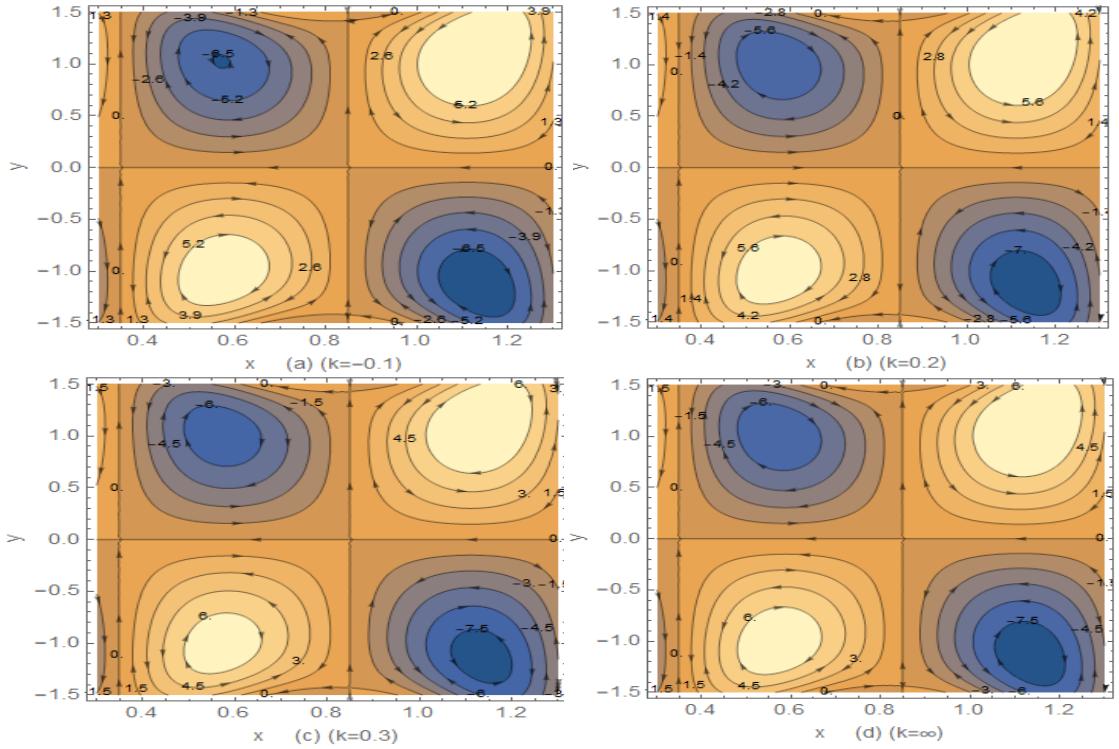

Figure 6: Stream Function $(t = 0.1, \mathrm{E1} = 1.2, \mathrm{E2} = 0.5, \mathrm{E3} = 0.1, \epsilon = 0.15, M = 5, \mathrm{k} = 0.1, m = 0.2, \beta = 0.1, \mu = 2.0, \rho = 0.9, \Omega = 0.2)$

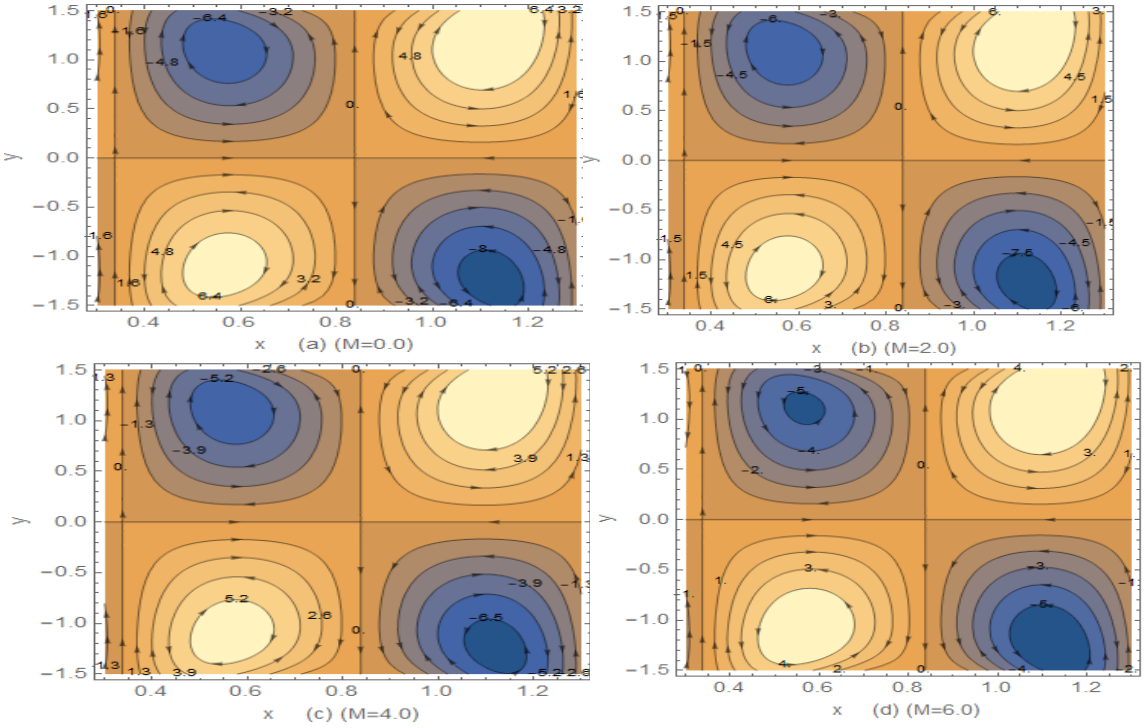

Figure 7: Stream Function $(t = 0.1, \mathrm{E1} = 0.7,\ \mathrm{E2} = 0.7,\ \mathrm{E3} = 0.7,\ \epsilon = 0.15,\ \mathrm{k} = 0.05,\ m = 0.25,\ \beta = 0.05,\ \mu = 2.0,\ \rho = 0.9,\ \Omega = 0.2)$.

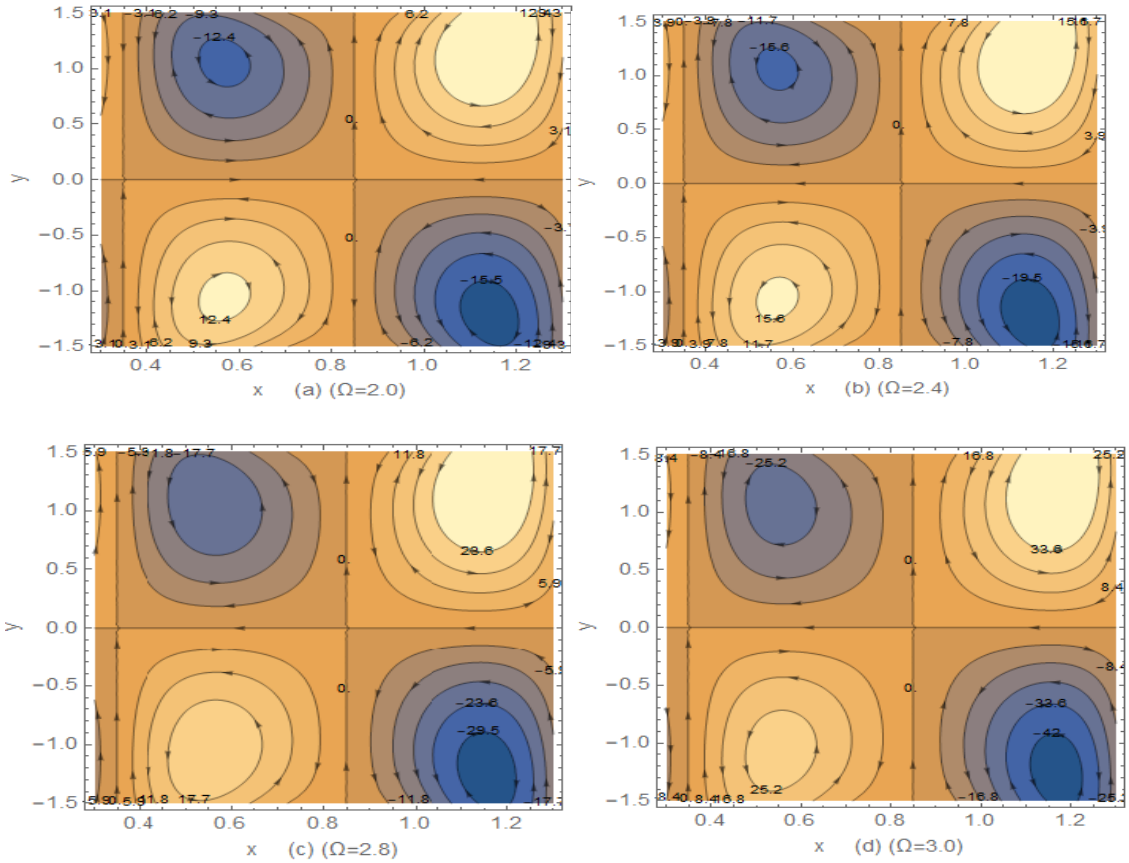

Figure 8: Stream Function ($t = 0.1$, E1 $= 1.2$, E2 $= 0.5$, E3 $= 0.1$, $\epsilon = 0.15$, $M = 2$, k $= 0.1$, $m = 0.25$, $\beta = 0.1$, $\mu = 2.0$, $\rho = 0.9$).

5. Conclusions

This study examines how the slip circumstances, rotation, and heat transmission affect the Peristaltic flow of MHD in porous channels when wall features are taken into consideration. The current investigation has the following observations:

1. When the value of the slip β and M increases, the magnitude of the axial velocity decreases at the channel's edges and center. On the other hand, we can see in the situations k, Ω, and m.
2. The temperature increases as the values of β, k, m, Ω, and BR grow, however, it decreases when M increases.
3. When the parameters β, k, Ω, and BR increase, the coefficient of the heat transfer increases as well; in contrast, when M, and m increase, the opposite occurs.
4. A decreasing number of boluses and an expansion of the bolus at the left of the channel are implied by the trapped bolus volume increasing with rotation value.
5. As the parameter k increases, the trapped bolus's volume grows. Additionally, more trapped bolus emerges.
6. This research can be used in applications in the digestive system, as well as the movement of food and waste within the intestine.

References

[1] A. Ebaid ," Effects of magnetic field and wall slip conditions on the peristaltic transport of a Newtonian fluid in an asymmetric channel", *Physics Letters A.* 2008, vol.372, pp:4493–4499.

[2] S. Srinivas, R. Gayathri, M. Kothandapani, "The influence of slip conditions, wall properties and heat transfer on MHD peristaltic transport", *Computer Physics Communications.* 2009, vol.180, pp: 2115–2122, https://doi.org/10.1016/j.cpc.2009.06.015.

[3] P. Lakshminarayana, S. Sreenadh and G. Sucharitha, "The Influence of Slip, Wall Properties on the Peristaltic Transport of a Conducting Bingham Fluid with Heat Transfer", Procedia Engineering. 2015 vol.127, pp: 1087-1094, http://creativecommons.org/licenses/by-nc-nd/4.0/.

[4] Zain Alabdeen A.N.ALSAFI, Ahmed A.H. Al-Aridhee and Saif Razzaq Al-Waily,"Effects of (MHD) and wall properties oscillatory flow for williamson fluid with constant viscosity through porous", *Wasit Journal of Computer and Mathematic Science.* 2021 vol. 1 no. 1.

[5] Abdelhalim Ebaid and Emad H. Aly, "Exact Analytical Solution of the Peristaltic Nanofluids Flow in an Asymmetric Channel with Flexible Walls and Slip Condition: Application to the Cancer Treatment", *Computational and Mathematical Methods in Medicine*. 2013, vol. 2013, Article ID 825376, http://dx.doi.org/10.1155/2013/825376.

[6] Batool A. Almusawi and Ahmed M. Abdulhadi, "Heat Transfer Analysis and Magnetohydrodynamics Effect on Peristaltic Transport of Ree–Eyring Fluid in Rotating Frame ", *Iraqi Journal of Science.* 2021, vol. 62, no. 8, pp: 2714-2725, DOI: 10.24996/ijs.2021.62.8.25.

[7] C. Rajashekhar, F. Mebarek-Oudina, H. Vaidya, K. V. Prasad, G. Manjunatha and H. Balachandra, "Mass and heat transport impact on the peristaltic flow of a Ree–Eyring liquid through variable properties for hemodynamic flow", wileyonlinelibrary.com/journal/htj. 2021, DOI: 10.1002/htj.22117.

[8] C. Rajashekhar, G. Manjunatha, F. Mebarek-Oudina, Hanumesh Vaidya,K.V. Prasad, K. Vajravelu and A.Wakif6, "Magnetohydrodynamic peristaltic flow of Bingham fluid in a channel: An application to blood f low", *JOURNAL OF MECHANICAL ENGINEERING AND SCIENCES.* 2021, vol. 15, ISSUE 2, pp: 8082 – 8094, DOI: https://doi.org/10.15282/jmes.15.2.2021.12.0637.

[9] M. Kothandapani and S. Srinivas, "On the influence of wall properties in the MHD peristaltic transport with heat transfer and porous medium", *Physics Letters.* 2008, vol.372, pp: 4586–4591.

[10] Mustafa, M. Hina, S. Hayat, T. Alsaedi, A., "Slip Effects on the Peristaltic Motion of Nanofluid in a Channel With Wall Properties", *Journal of Heat Transfe*. 2013, vol. 135,no.4, pp.041701, doi:10.1115/1.4023038.

[11] I. M. Eldesoky, R. M. Abumandour, M. H. Kamel and E. T. Abdelwahab, "The combined influences of heat transfer, compliant wall properties and slip conditions on the peristaltic flow through tube", *SN Applied Sciences.* 2019, vol.1, no.897,| https://doi.org/10.1007/s42452-019-0915-4.

[12] T. Hayat and S. Hina, "The influence of wall properties on the MHD peristaltic flow of a Maxwell fluid with heat and mass transfer", *Nonlinear Analysis: Real World Applications*. 2010, vol.11, pp: 3155-3169.

[13] A. Tanveer, M.Y. Malik, "Slip and porosity effects on peristalsis of MHD Ree-Eyring nanofluid in curved geometry", Ain Shams Engineering Journal. 2021, vol.12, pp: 955–968.

[14] N.M. Hafez, A.M. Abd-Alla, T.M.N. Metwaly, "Influences of rotation and mass and heat transfer on MHD peristaltic transport of Casson fluid through inclined plane", *Alexandria Engineering Journa.* 2023, vol. 68, pp:665-692, https://doi.org/10.1016/j.aej.2023.01.038.

[15] Hatem Nahi Mohaisen and Ahmed M. Abdalhadi, "Effects of The Rotation and A Magnetic Field on The Mixed Convection Heat Transfer Analysis for The Peristaltic Transport of Viscoplastic Fluid Through A Porous Medium in Asymmetric Channel", *J. Phys.: Conf. Ser.* 2021, 1963 012165, doi:10.1088/1742-6596/1963/1/012165.

[16] Hatem Nahi Mohaisen, Ahmed M.Abedulhadi, "Effects of the Rotation on the Mixed Convection Heat Transfer Analysis for the Peristaltic Transport of Viscoplastic Fluid in Asymmetric Channel", *Iraqi Journal of Science*. 2022, vol. 63, no. 3, pp: 1240-1257,

a. DOI: 10.24996/ijs.2022.63.3.29

[17] M. O. Kadhima, Liqaa Z. Hummady, "Effect of the rotation and inclined magnetic field on peristaltic slip flow of a Bingham fluid with heat transfer in asymmetric channel and porous medium", *Results in Nonlinear Analysis.* 2023, vol.6 no. 1, pp: 131–154, https://doi.org/10.31838/rna/2023.06.01.012.

[18] Y. Elmhed, A. Abd-Alla, M. Abdallah, "Effect of heat transfer and rotation on the peristaltic flow of a micropolar fluid in a vertical symmetric channel*", Sohag J. Sci.* 2022, vol.7, no. 3, pp: 117-122, https://dx.doi.org/10.21608/sjsci.2022.148710.1011.

[19] Hatem Nahi Mohaisen and Ahmed M.Abdalhadi," Influence of the Induced Magnetic and Rotation on Mixed Convection Heat Transfer for the Peristaltic Transport of Bingham plastic Fluid in an Asymmetric Channel", *Iraqi Journal of Science.* 2022, vol. 63, no. 4, pp: 1770-1785, DOI: 10.24996/ijs.2022.63.4.35.

[20] Rana Ghazi Ibraheem and Liqaa Zeki Hummady, "Effect of Different Parameters on Powell-Eyring Fluid Peristaltic Flow with the Influence of a Rotation and Heat Transform in an Inclined Asymmetric Channel", *Baghdad Science Journal*. September 2023, https://dx.doi.org/10.21123/bsj.2023.8360.

[21] Amaal Mohi Nassief and Ahmed M. Abdulhadi, "Peristaltic Transport of Non-Newtonian Fluid under Effects of Magnetic Force and Heat Transfer in a Symmetric Channel through a Porous Medium", *Baghdad Science Journal.* September 2023, https://dx.doi.org/10.21123/bsj.2023.7835.

[22] Rashid Ayub, Shahzad Ahmad and Mushtaq Ahmad, "MHD rotational flow of viscous fluid past a vertical plate with slip and Hall effect through porous media: A theoretical modeling with heat and mass transfer", *Advances in Mechanical Engineering*, 2022, vol. 14, no.6, pp: 1–14, https://doi.org/10.1177/16878132221103330.

[23] Hatem Nahi Mohaisen, "Influence of Rotation and Inclined Magnetic Field with Mixed Convective Heat and Mass Transfer in an Inclined Symmetric Channel on Peristaltic Flow with Slip Conditions", *Iraqi Journal of Science.* 2023, vol. 64, no. 12, pp: 6460- 6476. https:// DOI: 10.24996/ijs.2023.64.12.29.

[24] Sumithra R., Komala B, Manjunatha N., "Triple diffusive magneto convection in a fluid-porous composite system", *MATHEMATICAL MODELING AND COMPUTING*, 2023, vol. 10, no. 1, pp. 226–238, DOI: 10.23939/mmc2023.01.226.

[25] Yellamma, Manjunatha Narayanappa, Ramalingam Udhayakumar, Barakah Almarri, Sumithra Ramakrishna and Ahmed M. Elshenhab, "The Impact of Heat Source and Temperature Gradient on Brinkman–Bènard Triple-Diffusive Magneto-Marangoni Convection in a Two-Layer System", *Symmetry*, 2023, vol.15, 644. https://doi.org/10.3390/ sym15030644.